NANO LETTERS

2008
Vol. 8, No. 5
1417-1422

Colored Semitransparent Conductive Coatings Consisting of Monodisperse Metallic Single-Walled Carbon Nanotubes

Alexander A. Green and Mark C. Hersam*

Department of Materials Science and Engineering and Department of Chemistry, Northwestern University, Evanston, Illinois 60208-3108

Received January 30, 2008; Revised Manuscript Received March 12, 2008

ABSTRACT

Single-walled carbon nanotubes (SWNTs) are promising materials for transparent conduction as a result of their exceptional electrical, optical, mechanical, and chemical properties. However, since current synthetic methods yield polydisperse mixtures of SWNTs, the performance of SWNT transparent conductive films has previously been hindered by semiconducting species. Here, we describe the performance of transparent conductors produced using predominantly metallic SWNTs. Compared with unsorted material, films enriched in metallic SWNTs can enhance conductivity by factors of over 5.6 in the visible and 10 in the infrared. Moreover, by using monodisperse metallic SWNTs sorted with angstrom-level resolution in diameter, semitransparent conductive coatings with tunable optical transmittance can be produced.

Transparent conductive coatings are essential elements of flat panel displays, organic light-emitting diodes, solar cells, and electrochromic devices.[1,2] Despite the technological importance of transparent conductors, indium tin oxide (ITO), the most widely used material for these applications, has several weaknesses: (a) ITO is relatively brittle, which degrades its performance on flexible substrates; (b) ITO is increasingly expensive due to the limited availability of indium; (c) ITO has limited chemical stability leading to corrosion in device structures.[3] In response to these limitations, single-walled carbon nanotubes (SWNTs) have received increasing attention as a replacement transparent conductive material. These nanomaterials consist entirely of carbon, one of the most abundant elements, and have exceptional electrical,[4,5] optical,[6] mechanical,[7,8] and chemical[9,10] properties, which allow SWNT thin films to conduct on flexible substrates with strong environmental stability.

While there has been much progress in the development of SWNT transparent conductors in recent years,[11–13] previous work has been limited by the unavoidable polydispersity of as-produced SWNTs. This polydispersity stems from the unique structure of SWNTs which can be considered as graphene sheets rolled into seamless cylinders. Although this structure imbues SWNTs with their remarkable characteristics, it also renders their properties highly sensitive to the nanotube diameter and helicity. Of all possible SWNT chiralities, roughly one-third are metallic with the remainder being semiconductors whose bandgaps vary inversely with nanotube diameter. Despite efforts to synthesize SWNTs that are monodisperse in structure,[14,15] SWNT growth continues to produce material with a distribution of diameters and varying electronic character. As a result, previous work on transparent conductive SWNT networks has involved material with a preponderance of semiconducting SWNTs and optical characteristics defined by a broad distribution of SWNT diameters.

Herein, we employ a technique known as density gradient ultracentrifugation (DGU)[16–18] that addresses the SWNT polydispersity problem, thus enabling the production of transparent conductors consisting predominantly of metallic SWNTs with small diameter distributions. In the DGU process, SWNTs individually encapsulated in amphiphilic surfactant molecules are ultracentrifuged at high rotational frequency within a density gradient. Under these conditions, the SWNTs are driven to their isopycnic point in the gradient (i.e., the point where the SWNT density matches the density of the surrounding medium). Following ultracentrifugation, colored bands of sorted SWNTs can be recovered and incorporated directly into transparent conductive films. Films generated from sorted metallic SWNTs offer two major improvements over those produced from unsorted material. First, DGU eliminates poorly conducting, strongly absorbing carbonaceous impurities and semiconducting SWNTs to enhance transparent conductor electrical performance and optical transmissivity. Second, since the optical absorption

* Corresponding author. E-mail: m-hersam@northwestern.edu.

10.1021/nl080302f CCC: $40.75
Published on Web 04/08/2008

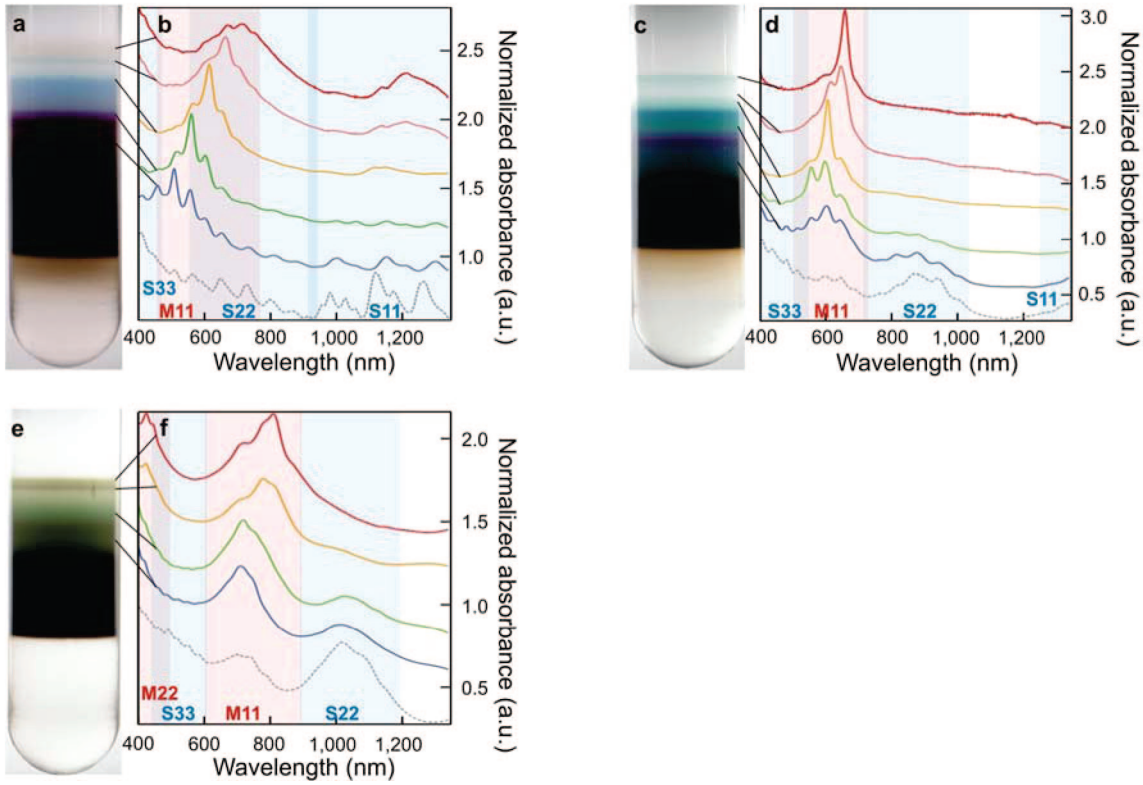

Figure 1. (a,c,e) Photographs of ultracentrifuge tubes following DGU. Colored bands of monodisperse metallic SWNTs are clearly visible for HiPco (a), laser-ablation (c), and arc discharge produced (e) SWNTs. (b,d,f) Sorted SWNTs (solid) were collected from gradients at points labeled by black lines and characterized using optical absorbance for comparison to unsorted material (dashed, gray). Wavelengths associated with first-, second-, and third-order semiconducting transitions (shaded blue) and first- and second-order metallic transitions (shaded red) are labeled S11, S22, S33, M11, and M22, respectively. Enrichment in metallic SWNT species is indicated in the sorted material by strong suppression of optical transitions associated with semiconducting SWNT species. (b) Metallic HiPco SWNTs can be sorted with diameters ranging from 0.7 to 1.3 nm, as evidenced by blue-shifting in the first-order optical transitions of the metallic SWNTs recovered progressively lower in the gradient. (d) For laser-ablation-synthesized material, DGU yields metallic SWNTs with diameters between 1.0 and 1.3 nm. The top three spectra demonstrate enrichment to greater than 98% purity, with each fraction possessing a different dominant SWNT diameter. (f) The arc discharge-grown SWNTs yield metallic nanotubes with the largest diameters, ranging from 1.4 to 1.7 nm.

of metallic SWNTs is strongly dependent on diameter, the angstrom-level control over nanotube diameter afforded by DGU results in films possessing a variety of different colors. These semitransparent conductive SWNT coatings offer an unprecedented degree of control over the optical properties of the transparent conductor. The transmittance of ITO, for instance, can only be controlled through film thickness and doping level and cannot be tuned with the fidelity that we report here for sorted SWNTs.[19] Accordingly, conductive SWNT coatings are expected to enhance transparent conductor performance in multiple applications. High transmittance regions of optimized films could be employed to increase the efficiency of devices such as flat panel displays, light emitting diodes, and solar cells. Conversely, the sharply peaked low transmittance regions of the coatings could be used to filter out unwanted portions of the optical spectrum that compromise device performance.

To generate bulk quantities of metallic SWNTs with a large range of diameters, we sorted SWNTs produced through three different synthetic routes: high pressure carbon monoxide conversion (diameter ~0.7−1.3 nm; HiPco; Carbon Nanotechnologies Inc., TX), laser-ablation (diameter ~1.1−1.4 nm; Carbon Nanotechnologies Inc., TX), and electric arc discharge (diameter ~1.3−1.7 nm; Carbon Solutions Inc., CA). For each of these starting materials, SWNTs dispersed in surfactants were concentrated and then ultracentrifuged in density gradients loaded with the surfactants sodium cholate (SC) and sodium dodecyl sulfate (SDS) mixed in a 3:2 SDS/SC ratio.[17] Following separation, highly refined metallic SWNTs having relatively low buoyant densities converged to multiple colored bands near the top of the density gradient corresponding to SWNTs with diameters ranging from 0.7 to 1.7 nm (Figure 1a,c,e). We achieved high resolution sorting of this large range of SWNT diameters by varying the overall loading of surfactants inside the gradients. While the mode of separation (metallic or semiconducting) is largely insensitive to changes in surfactant loading, modification of this parameter does affect the thickness of the surfactant shell surrounding the SWNTs. Since the buoyant density of a SWNT is strongly influenced by this surfactant shell, one can engineer larger differences in the buoyant density of SWNTs in a specific diameter range by controlling the surfactant loading and in turn can improve the diameter refinement provided by DGU. Independent of the surfactant level, the buoyant density of the metallic SWNTs in 3:2 SDS/SC environments is inversely related to

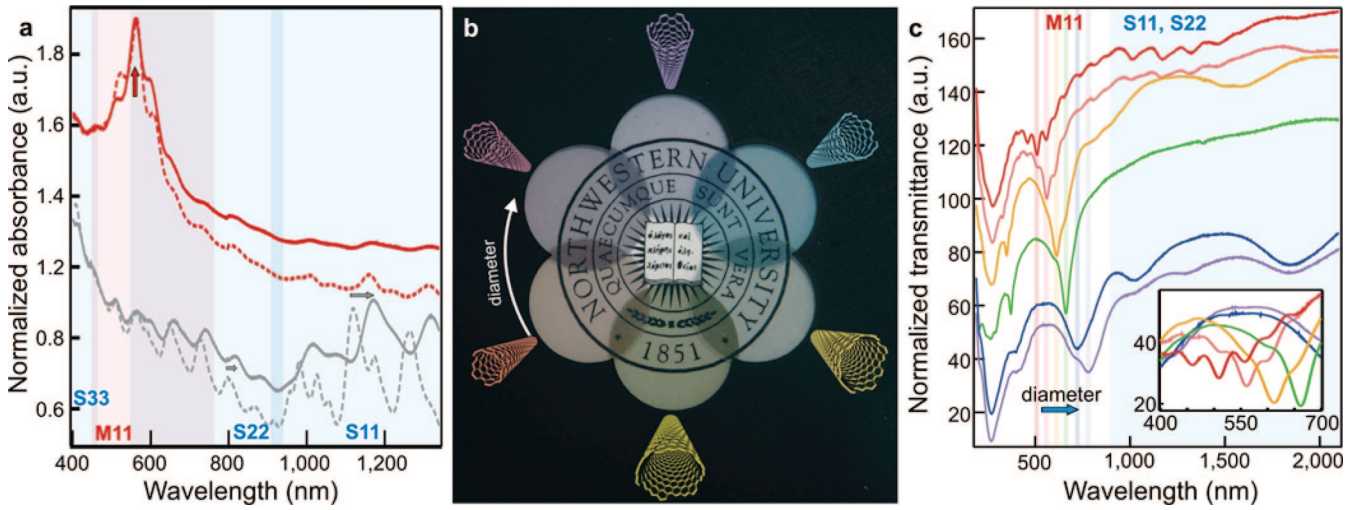

Figure 2. (a) Comparison of the absorbance of HiPco SWNT transparent conductive films (solid) with that of the SWNT dispersions (dashed) used to produce them (red and gray curves correspond to 1.0 nm diameter metallic and unsorted SWNTs, respectively; curves offset for clarity). While the bundling of SWNTs inside the films induces peak broadening and red-shifting of the semiconducting SWNT transitions (indicated by gray arrows), large peak shifts and broadening are not observed for metallic SWNT transitions (indicated by the red arrow). (b) Photograph of colored semitransparent conductors on PET under regular fluorescent lighting. The films are arranged in order of increasing mean diameter (clockwise starting from lower left): 0.9, 1.0, 1.05, 1.1, 1.4, and 1.6 nm. The transparency of the films is evidenced by the Northwestern University seal, which can be clearly seen through the films. (c) The transmittance of sorted metallic SWNT films normalized to the π-plasmon at approximately 270 nm (curves offset of clarity). The films were produced using SWNTs of the following dominant diameters (from top to bottom): 0.9, 1.0, 1.1, 1.3, 1.4, and 1.6 nm as implied by their first-order metallic transitions shifting from 509 to 778 nm. Inset: Magnified plot (same units) of the visible portion of the spectrum for the same SWNT films displaying optical tunability. Optical transitions are labeled following the conventions of Figure 1.

their diameter, with the largest diameter SWNTs banding at the top of the gradient and the smaller diameter material converging in progressively lower regions.

For the separation of HiPco SWNTs, we set the surfactant loading to 1.5% (w/v) to isolate metallic nanotubes with diameters centered about 1.0 nm (Figure 1a). The optical absorbance spectra of the bands removed from this gradient provide clear evidence of sorting by diameter and electronic type (Figure 1b). When compared with the starting HiPco material, the sorted metallic SWNTs show strong suppression of transitions beyond 600 nm associated with semiconducting SWNTs and the enhancement of those from 400 to 700 nm arising from metallic SWNTs. Furthermore, the isolation of metallic SWNTs with diameters ranging from 0.7 to 1.3 nm is evidenced by the shifts in their first-order optical transitions from 450 to 680 nm. DGU of laser-ablation-grown and arc discharge-produced SWNTs at surfactant loadings of 1.25% and 1%, respectively, result in metal sorting optimized for 1.2 and 1.5 nm diameters, respectively. As with HiPco material, separation by electronic type and diameter is evidenced by elimination of semiconducting optical transitions in the near-infrared and shifting of the first-order metallic transitions between 550 and 810 nm. Laser-ablation-produced SWNTs provide particularly refined sorting by electronic type and diameter. The top region of the density gradient (Figure 1c) yields material with greater than 98% metallic SWNT content (Figure 1d, Figure S1). For the arc discharge material, some of the first-order optical transitions of the metallic SWNTs appear in the near-infrared as a result of their large diameters. In addition, the second-order optical transitions of the 1.5 to 1.7 nm diameter material appear in the visible near 425 nm. Analysis of the optical absorbance spectra for the arc discharge SWNTs indicates that ~7.8% of metallic SWNTs initially inserted into the density gradients are recovered in fractions with greater than 86% metallic purity (see Supporting Information).

Following optical characterization, the monodisperse metallic SWNT solutions were incorporated into thin films through vacuum filtration and transferred to transparent substrates such as glass, quartz, and polyethylene terephthalate (PET).[11] During filtration, the surfactants encapsulating the SWNTs were removed by rinsing with copious amounts of water. The removal of surfactant causes the SWNTs to aggregate into bundles as a result of strong internanotube van der Waals interactions. Comparison of the absorbance of the transparent conductive SWNT films with that of the SWNT dispersions reveals substantial differences between the optical behavior of metallic and semiconducting SWNTs when they are highly bundled in films (Figure 2a). In the transparent conductive SWNT films, the first- and second-order transitions of the semiconducting species red-shift by approximately 40 and 30 meV, respectively, and broaden significantly. In contrast, the transitions associated with the dominant metallic SWNTs undergo a blue-shift of ~10 meV and exhibit relatively limited peak broadening. The reduced sensitivity to bundling for metallic SWNTs has been observed in solution for surfactant encapsulated bundles.[20] We attribute this effect to the increased charge screening capacity of metallic SWNTs, which reduces their sensitivity to changes in the external dielectric environment.

The ability of metallic SWNTs to retain their optical absorbance characteristics following film formation is beneficial for transparent conductive coatings as it ensures that films produced from sorted materials will possess definite

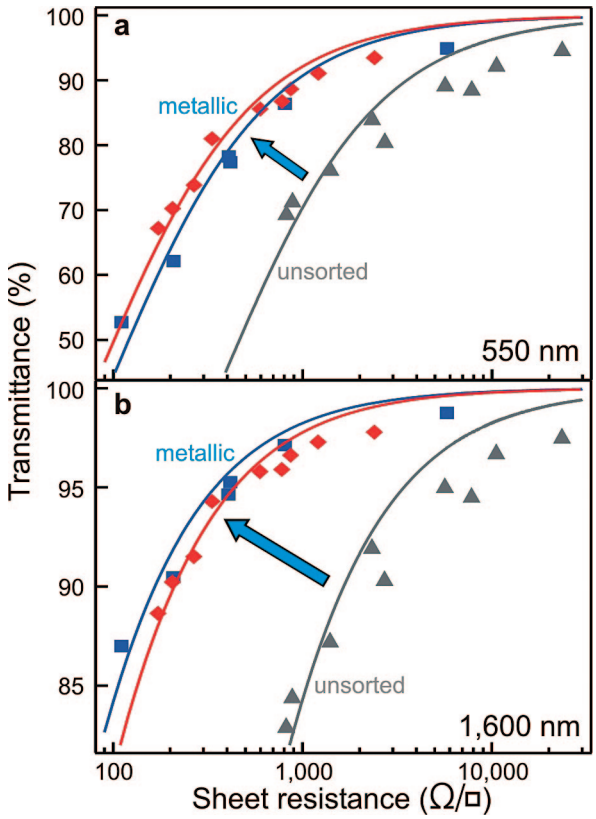

Figure 3. Transmittance versus sheet resistance for a series of transparent conductive films generated from HiPco SWNTs at 550 nm (a) and 1600 nm (b) wavelengths. The materials used were metallic SWNTs with principal diameters of 0.9 nm (red diamonds), 1.0 nm (blue squares), and unsorted material (gray triangles). The optical and electrical properties were related using eq 1 to generate the fitting curves. Improvements in the performance of metallic SWNTs versus unsorted SWNTs are observed with conductivity enhancement factors in excess of 5.6 in the visible and up to 10 in the infrared.

colors (Figure 2b). The high transmittance regions that define the colors of the transparent conductors can be tuned through most of the visible spectrum and into the near-infrared by control over the metallic SWNT diameters introduced into the film. To illustrate this capability, we have measured the transmittance spectra of a series of metallic SWNT films with dominant diameters ranging from 0.9 to 1.6 nm (Figure 2c). For these films, the first-order transitions vary from 509 to 778 nm, leaving high transmittance windows at wavelengths on either side of the absorption peak. Metallic SWNTs of 1.4 to 1.6 nm diameter, in particular, appear to be optimal chiralities for general purpose transparent conduction as their transmittance in the visible peaks around 550 nm, a wavelength range over which the human eye is the most sensitive and solar radiation is the most intense. Perhaps the most intriguing possibilities for colored SWNT coatings, however, lie in applications where high spectral selectivity is required. Given the insensitivity of the metallic nanotubes to bundling, it is possible to combine multiple monodisperse metallic SWNT samples to establish small regions of high transmittance and to effectively fill in the rest of the spectrum with absorbent SWNT chiralities to maximize film conductivity. Conversely, for semiconducting SWNTs, efforts to rationally shape the transmittance of thin films are likely to be confounded by large peak shifts and broadening associated with bundling.

In addition to improvements in film optical properties and transmittance tunability, we have observed enhancements in the conductivity of films generated from material enriched in metallic SWNTs compared with those of similar transparency made from unsorted SWNTs. To ensure valid comparisons, both sorted and unsorted HiPco SWNTs were processed in the same sonication batch (see Supporting Information) and, for several days prior to filtration, all SWNT dispersions were dialyzed into 1% SDS aqueous solutions. Prior to dialysis, large aggregates of SWNTs were removed from the unsorted material by ultracentrifugation at 288 000 g for 32 min. By subjecting the SWNTs to identical sonication conditions, we ensured that both the sorted and the unsorted nanotubes had identical length distributions, since SWNT buoyant density is insensitive to nanotube length[16] and sonication is known to shorten nanotubes by cutting them.[21] Centrifugation of the unsorted material as well as dialysis of both SWNT classes made certain that the sorted and unsorted nanotubes were in identical surfactant environments prior to film formation, which can affect the degree of bundling inside the film. After processing was complete, three sets of films were generated: one consisting of unsorted SWNTs and two containing monodisperse metallic SWNTs with dominant diameters of 0.9 and 1.0 nm, respectively.

Since the transparent conductive SWNT films have thicknesses lower than 100 nm, which is considerably shorter than optical wavelengths in the visible and infrared, the sheet resistance R_S of these films can be related to their transmittance at a given wavelength with the following equation:[12,22]

$$T = \left(1 + \frac{1}{2R_S}\sqrt{\frac{\mu_0}{\varepsilon_0}}\frac{\sigma_{op}}{\sigma_{dc}}\right)^{-2} \quad (1)$$

where σ_{op} is the optical conductivity which varies as a function of wavelength, σ_{dc} is the direct current conductivity, and μ_0 and ε_0 are the permeability and permittivity of free space, respectively. Equation 1 was used to fit the measured transmittance data for the transparent conductive films generated from HiPco SWNTs as shown in Figure 3. The films enriched in metallic SWNTs show clear reductions in sheet resistance compared with unsorted material. The improvement can be quantified by extracting the σ_{op}/σ_{dc} ratio obtained from the fits. For a series of films generated from a given SWNT material, this ratio determines the relationship between film transmittance and sheet resistance. Since σ_{op}/σ_{dc} is multiplied by the sheet resistance in eq 1, reductions in sheet resistance for unsorted and sorted SWNT material at a given transmittance level can be calculated by comparing σ_{op}/σ_{dc} for the corresponding series of films. In unsorted HiPco SWNT films, the average over visible wavelengths from 400 to 700 nm of σ_{op}/σ_{dc} is 1.1, in agreement with previously reported results.[22] Conversely, σ_{op}/σ_{dc} is 0.19 for metallic SWNT films in the visible, thus indicating a conductivity enhancement in excess of 5.6. Accordingly, a film of unsorted HiPco SWNTs will demonstrate a sheet resistance of ~1340 Ω/□ at 75% transmittance in the visible compared with a sheet resistance of ~231 Ω/□ for a film of

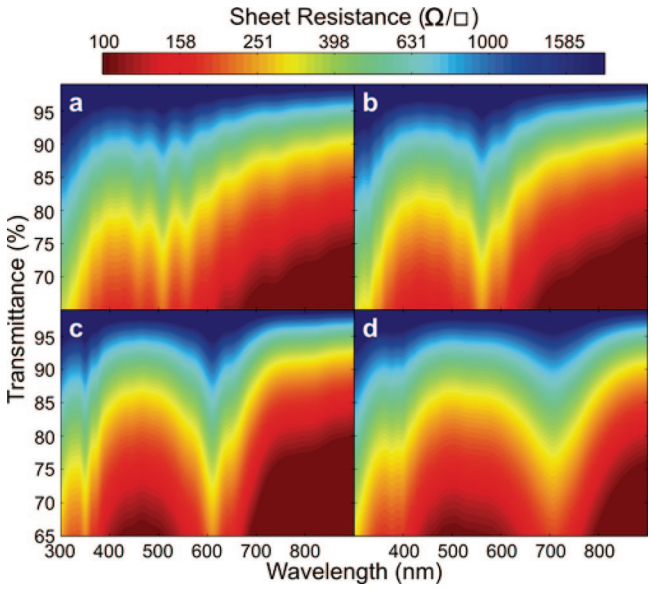

Figure 4. Sheet resistance-transmittance-wavelength maps of monodisperse SWNT conductive coatings. The color maps were generated by fitting eq 1 over several series of films: (a) 0.9 nm HiPco SWNTs, (b) 1.0 nm HiPco SWNTs, (c) 1.1 nm laser-ablation-grown SWNTs, and (d) 1.4 nm arc discharge-produced SWNTs.

sorted metallic HiPco SWNTs of the same transmittance. In the infrared from 800 to 2200 nm, the conductivity improvement exceeds 10 for metallic SWNTs of 1.0 nm diameter and 8.6 for 0.9 nm nanotubes. We attribute the smaller conductivity enhancement for 0.9 nm diameter SWNTs to increased semiconducting SWNT content which decreases film transmittance in the infrared.

The metallic SWNTs of monodisperse diameter generated by DGU, with their enhanced electronic and optical properties, effectively form a library of transparent conductor materials that can be selected and combined to achieve desired performance levels. To illustrate this concept, eq 1 was applied to transparent conductor data obtained from various metallic SWNT diameters over wavelengths from the ultraviolet to the infrared. The resulting sheet resistance-transmittance-wavelengths maps concisely describe the properties of the metallic SWNT transparent conductors (Figure 4). For applications requiring a particular transmittance level over a range of wavelengths, the sheet resistances of possible films can be obtained rapidly from these maps, thus easing the selection of optimal metal SWNT diameter.

The maps in Figure 4 also demonstrate that sorted SWNTs can produce sub-140 Ω/□ sheet resistance at transparencies greater than 70% in the visible and the near-infrared, which is sufficient for many applications. However, these maps also indicate that overall transparent conductor performance is related to the starting SWNT material. For both sorted and unsorted nanotubes, we have found that laser-ablation-grown SWNTs provide the best performance, followed by arc discharge material, and finally HiPco SWNTs. These differences in transparent conductor performance emphasize that the conductivity of SWNT thin films is determined by a variety of different factors such as SWNT length and nanotube−nanotube contacts, not simply the proportion of metallic SWNTs. We expect that film conductivity can be improved substantially by increasing the length of the sorted SWNTs either by using weaker sonication for dispersion or by using starting material consisting of longer SWNTs. Further increases in conductivity can be obtained by aligning the SWNTs in an effort to minimize scattering losses and to improve nanotube−nanotube contacts. A variety of methods such as dielectrophoresis,[23] tilted drop-casting,[24] and controlled flocculation[25] could be used to align the SWNTs along a preferred direction. Nevertheless, the marked increase in conductivity that we observe for metallic HiPco nanotubes over unsorted material in the absence of any other contributing factors is a promising finding that bodes well for future SWNT transparent conductors. Beyond modifying the length and morphology of SWNT films, much effort has been expended to dope SWNTs to improve their conductivity. However, such doping schemes are generally short-lived as a result of the limited thermal and chemical stability of doped SWNTs.[11,26] In contrast, transparent conductors formed from intrinsically conductive metallic SWNTs retain the excellent mechanical, thermal, and chemical properties of pristine carbon nanotubes.

In summary, we have generated the first SWNT transparent conductors consisting primarily of metallic SWNTs. These conductive coatings possess definite colors as a result of angstrom-level control over SWNT diameter and demonstrate conductivity increases by a factor of 5.6 in the visible spectrum and by a factor of 10 in the infrared spectrum over those produced from unsorted SWNTs. As longer SWNT sources become available, we expect that metallic SWNTs of monodisperse diameter will increasingly challenge ITO in transparent conductor applications, particularly those in which a high degree of optical tunability is required.

Acknowledgment. This work was supported by the U.S. Army Telemedicine and Advanced Technology Research Center (DAMD17−05−1−0381) and the National Science Foundation (DMR-0520513, EEC-0647560, and DMR-0706067). A Natural Sciences and Engineering Research Council of Canada Postgraduate Scholarship (A.A.G.) and an Alfred P. Sloan Research Fellowship (M.C.H.) are also acknowledged. Finally, the authors thank X. Du for sample preparation and measurement of optical absorbance, Q. H. Wang for assistance with photography of transparent conductive films, and M. S. Arnold and G. N. Ostojic for helpful discussions.

Supporting Information Available: Sample sonication, characterization, and analysis methods. This material is available free of charge via the Internet at http://pubs.acs.org.

References

(1) Lewis, B. G.; Paine, D. C. *MRS Bull.* **2000**, *25*, 22.
(2) Gruner, G. *J. Mater. Chem.* **2006**, *16*, 3533.
(3) Yang, Y.; Jin, S.; Medvedeva, J. E.; Ireland, J. R.; Metz, A. W.; Ni, J.; Hersam, M. C.; Freeman, A. J.; Marks, T. J. *J. Am. Chem. Soc.* **2005**, *127*, 8796.
(4) Dai, H. J.; Wong, E. W.; Lieber, C. M. *Science* **1996**, *272*, 523.
(5) Javey, A.; Guo, J.; Wang, Q.; Lundstrom, M.; Dai, H. J. *Nature* **2003**, *424*, 654.
(6) Arnold, M. S.; Sharping, J. E.; Stupp, S. I.; Kumar, P.; Hersam, M. C. *Nano Lett.* **2003**, *3*, 1549.

(7) Wong, E. W.; Sheehan, P. E.; Lieber, C. M. *Science* **1997**, *277*, 1971.
(8) Yu, M. F.; Lourie, O.; Dyer, M. J.; Moloni, K.; Kelly, T. F.; Ruoff, R. S. *Science* **2000**, *287*, 637.
(9) Hirsch, A. *Angew. Chem., Int. Ed.* **2002**, *41*, 1853.
(10) Niyogi, S.; Hamon, M. A.; Hu, H.; Zhao, B.; Bhowmik, P.; Sen, R.; Itkis, M. E.; Haddon, R. C. *Acc. Chem. Res.* **2002**, *35*, 1105.
(11) Wu, Z. C.; Chen, Z. H.; Du, X.; Logan, J. M.; Sippel, J.; Nikolou, M.; Kamaras, K.; Reynolds, J. R.; Tanner, D. B.; Hebard, A. F.; et al. *Science* **2004**, *305*, 1273.
(12) Zhou, Y. X.; Hu, L. B.; Gruner, G. *Appl. Phys. Lett.* **2006**, *88*, 123109.
(13) Ma, W. J.; Song, L.; Yang, R.; Zhang, T. H.; Zhao, Y. C.; Sun, L. F.; Ren, Y.; Liu, D. F.; Liu, L. F.; Shen, J.; et al. *Nano Lett.* **2007**, *7*, 2307.
(14) Kitiyanan, B.; Alvarez, W. E.; Harwell, J. H.; Resasco, D. E. *Chem. Phys. Lett.* **2000**, *317*, 497.
(15) Lolli, G.; Zhang, L. A.; Balzano, L.; Sakulchaicharoen, N.; Tan, Y. Q.; Resasco, D. E. *J. Phys. Chem. B* **2006**, *110*, 2108.
(16) Arnold, M. S.; Stupp, S. I.; Hersam, M. C. *Nano Lett.* **2005**, *5*, 713.
(17) Arnold, M. S.; Green, A. A.; Hulvat, J. F.; Stupp, S. I.; Hersam, M. C. *Nature Nanotech.* **2006**, *1*, 60.
(18) Green, A. A.; Hersam, M. C. *Mater. Today* **2007**, *10*, 59.
(19) Granqvist, C. G.; Hultaker, A. *Thin Solid Films* **2002**, *411*, 1.
(20) Huang, H. J.; Kajiura, H.; Maruyama, R.; Kadono, K.; Noda, K. *J. Phys. Chem. B* **2006**, *110*, 4686.
(21) Heller, D. A.; Mayrhofer, R. M.; Baik, S.; Grinkova, Y. V.; Usrey, M. L.; Strano, M. S. *J. Am. Chem. Soc.* **2004**, *126*, 14567.
(22) Hu, L.; Hecht, D. S.; Gruner, G. *Nano Lett.* **2004**, *4*, 2513.
(23) Krupke, R.; Hennrich, F.; von Lohneysen, H.; Kappes, M. M. *Science* **2003**, *301*, 344.
(24) Ko, H.; Tsukruk, V. V. *Nano Lett.* **2006**, *6*, 1443.
(25) Meitl, M. A.; Zhou, Y. X.; Gaur, A.; Jeon, S.; Usrey, M. L.; Strano, M. S.; Rogers, J. A. *Nano Lett.* **2004**, *4*, 1643.
(26) Li, Z. R.; Kandel, H. R.; Dervishi, E.; Saini, V.; Biris, A. S.; Biris, A. R.; Lupu, D. *Appl. Phys. Lett.* **2007**, *91*, 053115.

NL080302F